Medicinal Chemistry Research (2019) 28:1618–1627
https://doi.org/10.1007/s00044-019-02398-2

MEDICINAL CHEMISTRY RESEARCH

ORIGINAL RESEARCH

Check for updates

Design, synthesis, and biological evaluation of matrine derivatives possessing piperazine moiety as antitumor agents

Yiming Xu[1] · Pengyun Liang[1] · Haroon ur Rashid[1,2] · Lichuan Wu[3] · Peng Xie[1] · Haodong Wang[1] · Shuyan Zhang[1] · Lisheng Wang[3] · Jun Jiang[1]

Received: 20 April 2019 / Accepted: 10 July 2019 / Published online: 20 July 2019
© Springer Science+Business Media, LLC, part of Springer Nature 2019

Abstract

Using matrine (1) as the lead compound, a series of new piperazinyl matrine derivatives were designed, synthesized and evaluated for their antitumor activities in vitro and in vivo. Structure activity relationship (SAR) analysis indicated that introduction of substituted piperazine on matrine might significantly enhance the antiproliferative activity. Moreover, types of substituents of piperazine exhibited great different effects on the antiproliferative activity of target compounds against Bel-7402 and RKO cell lines. The in vivo antitumor assay results revealed that some of the target derivatives possessed better therapeutic efficacy than matrine and low toxicity. More importantly, among the newly synthesized compounds, **M16** and **M26** possessed strong antitumor activity against the two cell lines. Moreover, six of the synthesized compounds **M1**, **M3**, **M7**, **M10**, **M11** and **M17** proved to be of much better therapeutic efficacy than matrine via in vivo antitumor assay. The study provides a theoretical basis for further structural optimizations and discovery of the antitumor pathways of this kind of compounds.

Keywords Piperazine · Matrine · Antiproliferative activity · Cisplatin

Introduction

Malignant tumors continue to be a serious threat to human health. Currently, radiotherapy, chemotherapy and surgery are the major clinical techniques used to treat cancer. However, these techniques are extremely painful and cause serious side effects to the patients (Hamdy 2012). As a traditional means, tumor treatment through traditional Chinese medicine has attained significant attention due to their improved efficacy and low side effects. Matrine (1, Fig. 1), isolated from the natural herb-Sophora, has attracted considerable attention because of its broad-spectrum biological activities, including antitumor, anti-inflammatory, antiviral and anti-nociceptive effects (Zhang et al. 2010; Aghvami et al. 2018; Dai et al. 2009). Moreover, it has a flexible structure and good safety profiles. However, matrine has not been widely used in clinics as antitumor agent, but it has served as an adjuvant therapy in combination with chemotherapeutic or targeted anticancer agents in clinical cancer treatment, such as with cisplatin (Zhang et al. 2015) and sorafenib (Lin et al. 2014). Low bioavailability and moderate antitumor activity limited its application in tumor treatment. Thus, it is highly desirable to develop matrine derivatives in order to discover more effective drug candidates.

Piperazine scaffold has been recognized as one of the privileged structures in drug discovery and is widely distributed in biologically active compounds applied in a number of different therapeutic areas, including antitumor, antifungal, antidepressant, and antiviral (Solomon et al. 2010; Kimura et al. 2004; Shapiro et al. 1995; Yang et al. 2005).

These authors contributed equally: Yiming Xu, Pengyun Liang

Supplementary information The online version of this article (https://doi.org/10.1007/s00044-019-02398-2) contains supplementary material, which is available to authorized users.

✉ Lisheng Wang
lswang@gxu.edu.cn

✉ Jun Jiang
jiangjun@gxu.edu.cn

[1] School of Chemistry and Chemical Engineering, Guangxi University, Nanning 530004, China

[2] Department of Chemistry, Sarhad University of Science & Information Technology, PeshawarKhyber, Pakhtunkhwa 25120, Pakistan

[3] Medical College, Guangxi University, Nanning 530004, China

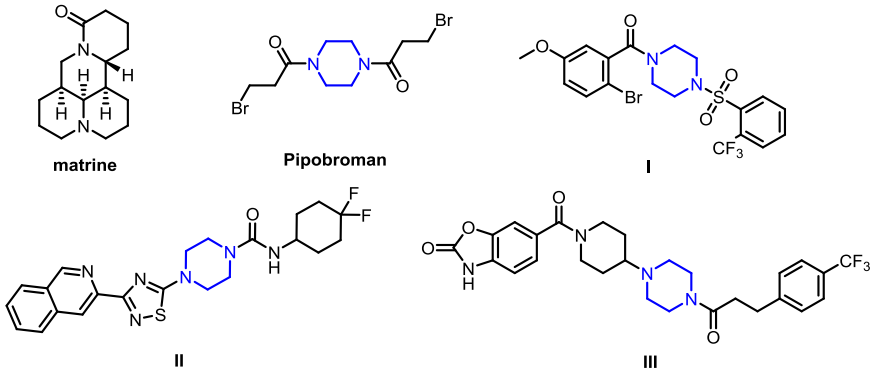

Fig. 1 Structures of matrine and piperazine derivatives as antitumor agents

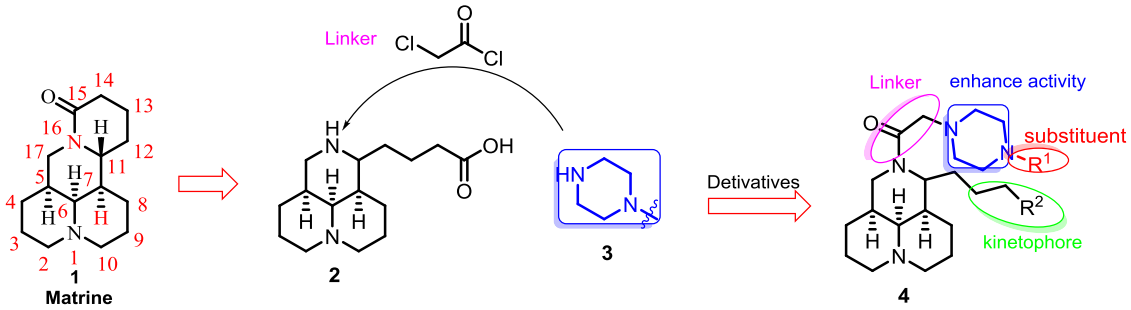

Scheme 1 Modification strategy of matrine with piperazine moiety

Piperazine can exert the improvement in pharmacokinetic features of drug candidates due to its two primary nitrogen atoms useful for maintaining appropriate pKa (Lacivita et al. 2009). Moreover, strong evidences support the fact that piperazine derivatives exhibit potent anticancer activities. Fajas et al. (Fajas et al. 2011) reported the use of drug **I** as an inhibitor of the expression and activity of hSCD enzymes especially SCD-1 and selective agent for blocking prostate cancer cells. Jones et al. (Jones et al. 2011) reported anticancer piperazine derivative **II** as SMO antagonist. Schiemann et al. (Schiemann et al. 2010) invented a highly potent analogue **III** as autotaxin inhibitor, useful for the treatment and prophylaxis of cancers such as malignant/solid/benign tumors, Ewing/Kaposi scarcomas, brain tumors, tumors associated with nervous system and hyperproliferative disorders as well as other autotaxin-mediated diseases.

Encouraged by the above results, we hypothesize that the introduction of piperazine scaffold on matrine could improve the antiproliferative activity of new analogs. In particular, new derivatives could have a significant impact on pharmacokinetics and pharmacodynamics, thereby, playing a crucial role in the bioavailability. Furthermore, slight modification in the substitution pattern on the pipeazine nucleus facilitates a considerable difference in the medicinal potential of the resultant molecules. Moreover, this type of modification is also a standard drug design scheme (Rathi et al. 2016). Herein, piperazine scaffold with substituents has been employed to develop structural modification of matrine substrate (Scheme 1).

Results and discussion

Chemistry

Twenty-seven target compounds were synthesized using commercially available matrine as a starting material by connecting it with substituted piperazine derivatives. As depicted in the first synthetic route (Scheme 2), intermediate **2** was obtained through hydrolyzation of matrine in aqueous KOH by reflux. Then thionyl chloride was added to the alcohol to form ethyl chlorosulfate followed by reaction with intermediate **2**, which facilitates the esterification smoothly in relatively high yields and purity. The ^{1}H NMR spectra of **3a** displayed a singlet at δ 3.64 ppm due to methyl ester, while **3b** showed a triplet and a quartet at δ 1.22 and 4.09 ppm because of ethyl ester. The key intermediates **5a-5b** were obtained by the condensation of **3a-3b** with chloroacetyl chloride under slightly alkaline conditions. Finally, substituted piperazines directly connected to phenyl at N position were used as nucleophilic reagents to transform matrinic ester into desired product **M1-M16**. The ^{1}H NMR spectra of **M1-M16** displayed signal shift at 6–7 ppm (ArH), indicating the introduction of **6a-6k** to **5a-5b**. In order to increase the hydrophilicity of the synthesized

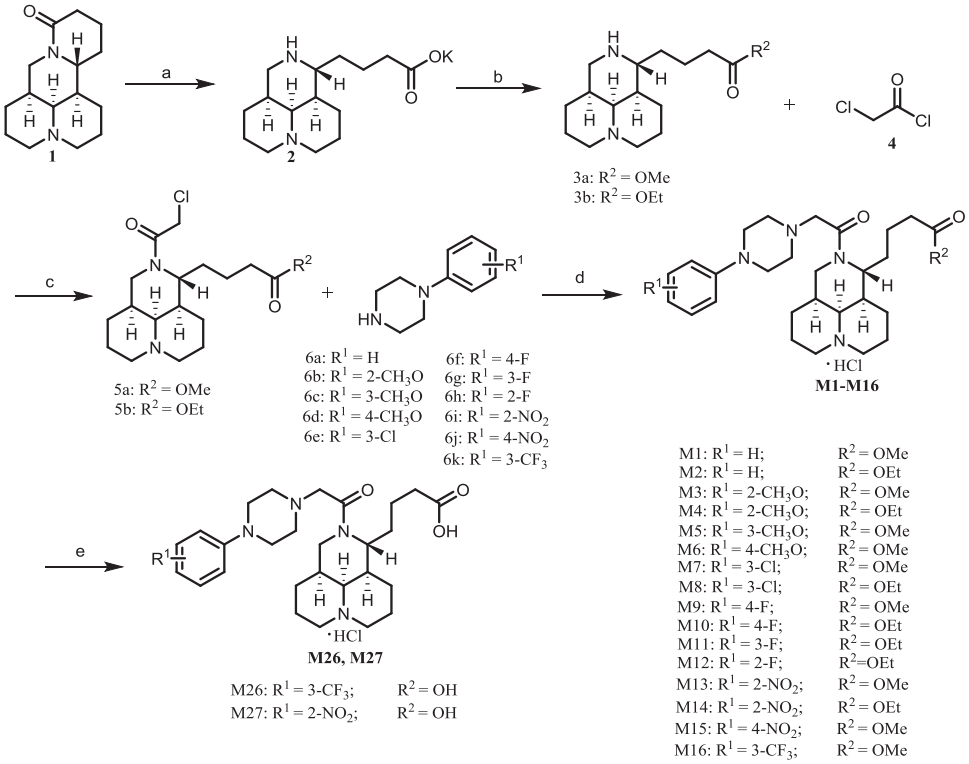

Scheme 2 Second synthetic route for matrine derivatives. Reactants and conditions: **a** KOH aqueous, 100 °C,12 h; **b** $SOCl_2$, CH_3OH/C_2H_5OH, reflux, 3 h; **c** K_2CO_3, acetone, rt, 3 h; **d** K_2CO_3, CH_3CN, reflux, 4 h; C_2H_5OH, HCl; **e** NaOH aqueous, rt, 1 h; C_2H_5OH, HCl

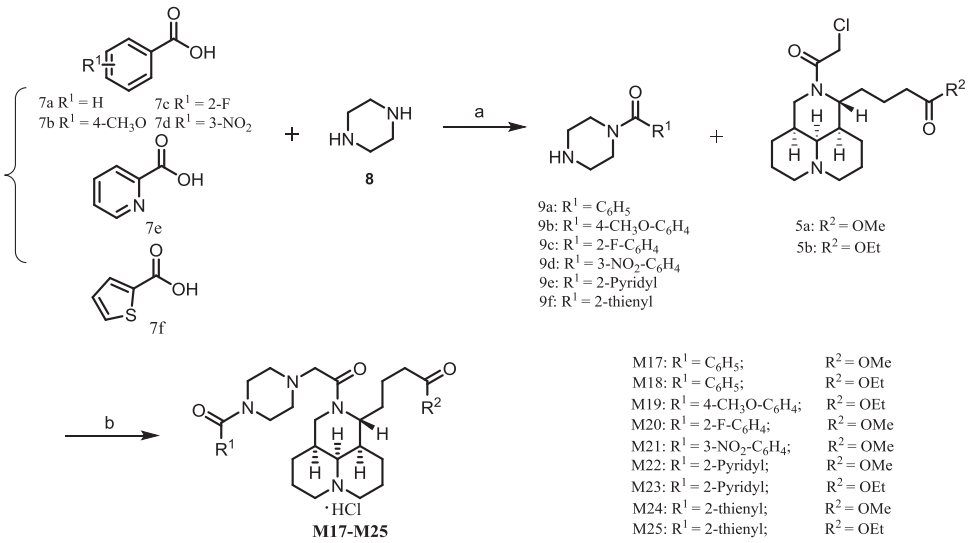

Scheme 3 Second synthetic route for matrine derivatives. Reactants and conditions: **a** $SOCl_2$, reflux, 2 h; rt, 30 min; **b** K_2CO_3, CH_3CN, reflux, 4 h; C_2H_5OH, HCl

analogs, the esters were also hydrolyzed to acids to produce **M26** and **M27**. The disappeared ^{1}H NMR signal of methyl ester of **M13** and **M16** when NaOH aqueous was added indicated the transformation to **M26** and **M27**.

In the second synthetic route (Scheme 3), a series of piperizine derivatives were first prepared via substitution reaction. Acids **7a-7f** were treated with thionyl chloride, and the corresponding acyl chlorides were subsequently allowed to react with piperizine to yield the monosubstituted **9a-9f** via controlled reaction rate. Finally, piperazine derivatives **9a-9f** were connected with the key intermediate **5a-5b** to produce target compounds **M17-M25**. The ^{1}H NMR spectra of **M17**-**M25** displayed signal shift at 6–7 ppm (ArH), indicating the connection between **9a**-**9f** with **5a**-**5b**. Moreover, the structures of **M17**-**M25** could be identified by mass spectrum.

Cell viability assay

The antiproliferative activities of the synthesized compounds against human hepatoma Bel-7402 and colorectal carcinoma RKO cells were evaluated through MTT assay

Table 1 Structures and cell viability of the twenty-seven matrine derivatives on 7402 and RKO cells

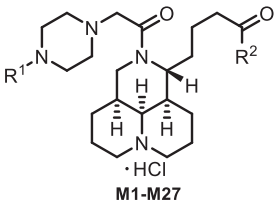

M1-M27

Compounds	R^1	R^2	Cell viability (%) at 50 μM	
			7402	RKO
matrine	–	–	86.6 ± 2.6	84.3 ± 2.5
M1	C_6H_5–	OMe	78.3 ± 2.1	81.7 ± 2.1
M2	C_6H_5–	OEt	71.3 ± 3.8	80.2 ± 2.4
M3	2-CH_3O-C_6H_4–	OMe	89.4 ± 2.2	83.8 ± 1.2
M4	2-CH_3O-C_6H_4–	OEt	85.2 ± 2.4	75.2 ± 2.6
M5	3-CH_3O-C_6H_4–	OMe	91.2 ± 3.4	88.0 ± 1.8
M6	4-CH_3O-C_6H_4–	OMe	88.3 ± 2.0	88.7 ± 3.1
M7	3-Cl-C_6H_4–	OMe	71.5 ± 2.5	76.1 ± 2.5
M8	3-Cl-C_6H_4–	OEt	72.3 ± 3.2	75.7 ± 2.7
M9	4-F-C_6H_4–	OMe	78.4 ± 3.2	79.8 ± 2.2
M10	4-F-C_6H_4–	OEt	90.1 ± 0.2	79.1 ± 4.6
M11	3-F-C_6H_4–	OEt	79.9 ± 0.6	84.1 ± 3.4
M12	2-F-C_6H_4–	OEt	75.9 ± 1.3	72.4 ± 3.8
M13	2-NO_2-C_6H_4–	OMe	84.3 ± 3.5	53.4 ± 1.8**
M14	2-NO_2-$C_6H_4^-$	OEt	78.1 ± 4.1	43.8 ± 2.5**
M15	4-NO_2-$C_6H_4^-$	OMe	73.3 ± 2.8	58.1 ± 3.7*
M16	3-CF_3-$C_6H_4^-$	OMe	50.4 ± 1.4**	48.3 ± 3.1**
M17	C_6H_5-CO–	OMe	81.2 ± 4.8	78.1 ± 2.0
M18	C_6H_5-CO–	OEt	78.8 ± 2.2	82.6 ± 2.4
M19	4-CH_3O–C_6H_4–CO–	OMe	76.1 ± 2.6	87.5 ± 4.8
M20	2-F-C_6H_4-CO–	OMe	81.1 ± 4.3	81.5 ± 2.7
M21	3-NO_2-C_6H_4-CO–	OMe	50.6 ± 2.5**	81.1 ± 1.4
M22	2-Pyridyl-CO–	OMe	72.2 ± 5.4	55.2 ± 1.3**
M23	2-Pyridyl-CO–	OEt	73.3 ± 2.3	76.2 ± 2.7
M24	2-thienyl-CO–	OMe	62.6 ± 3.4*	76.7 ± 3.5
M25	2-thienyl-CO–	OEt	61.3 ± 0.2*	75.8 ± 1.2
M26	3-CF_3-C_6H_4–	OH	48.3 ± 2.5**	51.3 ± 3.3**
M27	2-NO_2-C_6H_4–	OH	73.5 ± 2.1	56.2 ± 2.3*
Cisplatin	–	–	92.5 ± 1.6	68.0 ± 1.3

Compared with matrine, *$P < 0.05$; **$P < 0.01$

using cisplatin as a positive control. Structures of twenty-seven piperazinyl matrine derivatives and their cytotoxicity were shown in Table 1.

SAR analysis was focused on the substituents at the nitrogen atom of piperizine. In this part, phenyl group was first introduced upon nitrogen atom, resulting in the formation of **M1** and **M2** which were then tested. As indicated in Table 1, **M1** and **M2** showed a weak activity with their inhibition rates less than 30% at a concentration of 50 μM. Then, phenyl groups carrying electron-withdrawing and electron-donating moieties were subsequently connected with the nitrogen atom, following the produce of **M3-M12**. The cell viability results of the compounds **M3-M12** suggested that the electrophilic effect might be helpful to improve the antiproliferative activity. Hence, a series of N-substituted derivatives with the improved electrophilic effect was then obtained, aiming to enhance the antitumor activity. As expected, the results indicated that compounds **M13-M16** exhibited significantly higher cytotoxicity against RKO. Notably, **M16** exhibited potent activity against Bel-7402 and RKO cell lines simultaneously.

Next, we retained the substituent on the phenyl group, and replaced the linked group with acyl between benzene and piperizine to explore the SAR of the variation. Consequently, **M17-M21** were synthesized and tested. The most striking difference is that **M21** dispalyed potent activity only against Bel-7402 rather than RKO, showing different behavior with compounds **M13-M15**. Since some heterocyclic molecules have a promising application in antitumor field, so phenyl group was transformed into pyridyl and thienyl group to obtain **M22-M25**. The cytotoxicity results indicated that **M22** exhibited potent activity against RKO, while thienyl selectively improved the antitumor activity against Bel-7402.

In another variation, SAR study was carried out to investigate the kinetophore for the activity, and R^2 with methyl ester, ethyl ester and carboxylic acid were prepared. The results showed that there existed difference to a varying degree in the potency of target compounds caused by the kinetophore. It is noteworthy that the **M22** showed more potent activity than **M23** against RKO, suggesting that methyl ester group might play a more important role in improving the antitumor activity of these compounds.

Among the newly synthesiszed compounds, **M16** and **M26** showed potent antitumor activity against Bel-7402 and RKO, suggesting the importance of trifluoromethyl group and the possibility of the two target compounds as antitumor agents.

Antitumor activity in vivo

As shown in Table 2, most tested compounds exhibited higher antitumor activities than that of matrine to some extent, indicating the important of substituted piperazine. The value of tumor weight of all the compounds has obvious change compared to the vehicle group, indicating that all the compounds could reduce the tumor weight to some degree. After treatment with CTX, the observed toxicity was demonstrated by the absence of weight loss (thymus index and spleen index). However, the index of

Table 2 The in vivo antitumor activities of target compounds investigated in H22 tumor-bearing mice models

Groups	Numbers	Dose (mg/kg)	Thymus index	Spleen index	Tumor weight (g)	Inhibition (%)
Vehicle	10	–	30.78 ± 2.46	108.37 ± 5.12	1.55 ± 0.26	–
matrine	10	60	31.17 ± 2.18	113.54 ± 5.59	0.82 ± 0.19*	47.09
M1	10	60	31.29 ± 2.14	112.46 ± 4.74	0.71 ± 0.24*#	54.19
M2	10	60	30.73 ± 1.97	111.58 ± 5.57	0.80 ± 0.23*	47.99
M3	10	60	30.28 ± 2.18	113.36 ± 4.74	0.69 ± 0.16*#	55.45
M4	10	60	30.34 ± 1.93	109.27 ± 4.13	0.75 ± 0.22*	51.28
M5	10	60	30.32 ± 2.08	112.68 ± 4.98	0.73 ± 0.31*	52.46
M6	10	60	31.22 ± 2.27	112.56 ± 5.71	0.79 ± 0.22*	49.01
M7	10	60	30.28 ± 1.96	111.14 ± 5.17	0.66 ± 0.21*#	56.8
M8	10	60	30.16 ± 1.57	112.67 ± 5.45	0.78 ± 0.21*	49.17
M9	10	60	29.41 ± 1.84	112.39 ± 5.46	0.78 ± 0.20*	49.17
M10	10	60	30.25 ± 2.17	112.45 ± 4.86	0.67 ± 0.24*#	56.78
M11	10	60	30.26 ± 2.05	114.27 ± 4.85	0.70 ± 0.25*#	54.56
M12	10	60	30.42 ± 2.52	110.72 ± 5.75	0.79 ± 0.34*	49.01
M13	10	60	30.31 ± 2.06	110.51 ± 4.94	0.74 ± 0.26*	52.25
M14	10	60	29.98 ± 1.95	110.25 ± 5.42	0.81 ± 0.14*	47.74
M15	10	60	29.56 ± 1.95	111.55 ± 5.81	0.79 ± 0.22*	49.01
M16	10	60	31.28 ± 2.05	112.79 ± 5.06	0.79 ± 0.28*	49.01
M17	10	60	30.57 ± 1.89	110.58 ± 5.53	0.69 ± 0.28*#	55.35
M18	10	60	30.38 ± 1.86	112.89 ± 4.64	0.80 ± 0.32*	47.99
M19	10	60	29.75 ± 2.06	110.74 ± 5.13	0.79 ± 0.23*	49.01
M20	10	60	30.55 ± 2.11	111.25 ± 5.34	0.75 ± 0.21*	51.28
M21	10	60	31.69 ± 2.05	114.71 ± 4.95	0.82 ± 0.24*	47.09
M22	10	60	30.81 ± 2.07	109.96 ± 4.21	0.78 ± 0.22*	49.17
M23	10	60	29.75 ± 1.95	110.34 ± 4.36	0.76 ± 0.19*	50.57
M24	10	60	28.55 ± 1.91	112.28 ± 5.85	0.78 ± 0.25*	49.17
M25	10	60	29.52 ± 2.25	110.22 ± 5.26	0.79 ± 0.30*	49.01
M26	10	60	29.17 ± 2.35	112.54 ± 5.23	0.73 ± 0.20*	52.46
M27	10	60	30.16 ± 1.98	110.25 ± 5.01	0.81 ± 0.31*	47.74
CTX	10	30	26.21 ± 2.03*	62.64 ± 4.35*	0.57 ± 0.21*#	63.22

Compared with vehicle, $^{*}P < 0.05$; compared with matrine, $^{\#}P < 0.05$

matrine and its derivatives were the same to that of the vehicle. The results showed that matrine derivatives exhibited safer druggable advantages than CTX in vivo. Moreover, most of the derivatives exhibited more marked therapeutic efficacy than matrine. Among the synthesized compounds, **M1**, **M3**, **M7**, **M10**, **M11** and **M17** could effectively reduce the tumor weight. The results indicated that the substituents and their position on phenyl of R^1 and the variation of R^2 could take a great role in antitumor activity. Also, we speculated that the inconsistency between in vivo and in vitro activity of the compounds might associate with the pharmacological properties, such as drug absorption, metabolism etc. In general, the in vivo antitumor assay results indicated that some of the target compounds could serve as promising antitumor agents with little toxicity.

Conclusion

In summary, by conjugation of piperazine moiety with matrine, twenty-seven novel matrine derivatives were designed, synthesized and evaluated for antiproliferative activity against Bel-7402 and RKO and *in vivo* antitumor activity with H22 tumor-bearing mice models. Most of the synthesized compounds showed better anti-proliferative activity than matrine. After screening, it was observed that compounds **M16** and **M26** possessed strong antitumor activity against the two cell lines. Moreover, six of the synthesized compounds **M1**, **M3**, **M7**, **M10**, **M11** and **M17** proved to be of much better therapeutic efficacy than matrine via in vivo antitumor assay. Thus, the substituent piperazine moiety could enhance antiproliferative activity and in vivo antitumor activity to some certain compounds.

The inconsistency of efficacy between the anti-proliferative and in vivo activity of the compounds might be caused by pharmacological changes due to the introduction of piperazine moiety. Possible mechanisms of action of these compounds and the role of piperazine need further study. Taken together, the information gathered from this promising preliminary study may provide the basis and scientific evidence about the usefulness of piperazine as a moiety in matrine modification for antitumor treatment.

Materials and methods

Materials and instrumentation

Matrine was purchased from Shanxi Undersun Biomedtech Co., Ltd. All other chemicals and reagents used in the experiments were of analytical grade and obtained from Sinopharm Chemical Reagent Co., Ltd. Operation process was monitored by Thin Layer Chromatography (TLC) obtained from Yantai Xinnuo chemical Co. Ltd., and then visualized by UV light (254 nm) or Wagner's reagent. Column chromatography, equipped with commercial silica gel (300–400 mesh) obtained from Anhui LiangChen Silicon Material Co. Ltd, was performed for purification. Melting points were measured in open glass capillaries on X-4 melting-point apparatus (China) and are uncorrected. IR spectra were recorded on a PerkinElmer FI-IR-8400S spectrometer Spectrum. 1H-NMR spectra was recorded on Bruker Avance 600 (600 MHz) spectrometer (Brucker, Inc., Silberstreifen, Rheinstetten, Germany) with $CDCl_3$ as solvent. Chemical shifts (δ) are reported in ppm with Tetramethylsilane (TMS) as internal standard, coupling constants (J) are reported in hertz (Hz). Mass spectra were obtained from a GC-MS/QP5050A (ESI). Finally the optical density was measured at the 490 nm wavelength on an enzyme-linked immunosorbent assay microplate reader.

General experimental procedures

Synthesis of compounds 3a-3b

Matrine **(1)** (10 g, 40.3 mmol) and KOH (42 g, 0.75 mol) dissolved in H_2O (120 mL) were added to a 250 mL three-necked flask, then heated to reflux for 12 h. After completion of the reaction, the reactant was cooled to room temperature and filtered to get white solid as a product **2** in the yield of 86%. $SOCl_2$ (6 mL) was added to methanol/ethanol (40 mL) and stirred for 30 min in ice-bath and product **2** was then added portion-wise and the mixture was then refluxed for 3 h. After completion of the reaction, the mixture was filtered and solvent was concentrated to obtain **3a/3b**.

3a: white solid, yield: 82%, ^{1}H NMR (600 MHz, CD_3Cl) *δ*: 1.37–1.46 (m, 3H), 1.48–1.68 (m, 7H), 1.73–1.80 (m, 1H), 2.83–2.03 (m, 3H), 2.14 (s, 1H), 2.29–2.44 (m, 3H), 2.73–3.79 (m, 2H), 3.03–3.06 (dd, J = 4.2 Hz, J = 12 Hz, 1H), 3.41 (t, J = 12.6 Hz, 1H), 3.56–3.62 (m, 1H), 3.64 (s, 3H); IR (KBr) *ν*: 3474, 2942, 1728, 1440, 1397; ESI-MS, *m/z*: 279 {(M-1)}.

3b: white solid, yield: 79%, ^{1}H NMR (600 MHz, CD_3Cl) *δ*: 1.22 (t, J = 7.2 Hz, 3H), 1.35–1.66 (m, 8H), 1.73–1.81 (m, 1H), 1.87–2.01 (m, 7H), 2.14 (s, 1H), 2.31–2.41 (m, 3H), 2.73–3.79 (m, 2H), 3.04–3.07 (dd, J = 4.2 Hz, J = 12 Hz, 1H), 3.41 (t, J = 12.6 Hz, 1H), 3.58–3.61 (m, 1H), 4.09 (q, J = 7.2 Hz, 2H); IR (KBr) *ν*: 3437, 2948, 1728, 1473, 1403; ESI-MS, *m/z*: 294 {(M + 1)}.

Synthesis of compounds 5a-5b

K_2CO_3 (1.38 g, 10 mmol) was added to a solution of **3a/3b** (5 mmol) in acetone (25 mL). To this solution chloroacetyl chloride was added by droping at 0 °C. The mixture was stirred for 3 h at 35 °C. Then water (100 mL) was added to the reaction mixture followed by its extraction with ethyl actate (3 × 20 mL). The organic phase was dried using sodium sulfate, filtered and removed under vacuum to obtain crude products **5a/5b** in the yield of 72%. The products were used for the next step without further purification.

Synthesis of compounds 9a-9f

A mixture of commercial carboxylic acid **7a-7f** (1 mmol) in freshly distilled thionyl chloride was heated to reflux for 2 h, then cooled to room temperature and evaporated under vacuum to dryness to afford quantitatively corresponding acid chlorides. The acid chlorides were dissolved in dichloromethane, followed by the slow addition of a mixture of piperazine (86 mg, 1 mmol) and pyridine (197 mg, 2.5 mmol) at room temperature and stirring was continued for 30 min. After completion of reaction, the solvent was washed with aq. sodium bicarbonate. The organic layer was collected, dried with sodium sulfate, filtered and removed under vacuum to obtain products **9a-9f** without purification in the yields of above 90%.

Synthesis of compounds M1-M16, M17-M25

Compound **6a-6k** or **9a-9f** (1.2 mmol) and **5a-5b** (1 mmol) were dissolved in acetonitrile (25 mL), followed by the addition of K_2CO_3 (0.27 g, 2 mmol) to the solution. The mixture was heated to reflux for 4 h. The hot precipitate was filtered and the filtrate was evaporated under reduced pressure to get crude product, which was purified by

column chromatography on silica gel eluting with dichloromethane: methanol (50: 1~30:1) to afford oil products. Then a saturated solution of hydrochloric acid in ethanol was added to the products and concentrated to get final target compounds **M1-M16** and **M17-M25**.

M1: yellow powder; yield: 64%; m.p.: 190–192 °C; ^{1}H NMR (600 MHz, DMSO-d6) δ: 10.12–9.97 (m, 2H), 7.27 (t, J = 8.4 Hz, 2H), 7.03 (d, J = 8.4 Hz, 2H), 6.88 (t, J = 8.4 Hz, 1H), 4.82–4.80 (m, 1H),4.38 (d, J = 16 .2 Hz, 1H), 4.21–4.15 (m, 1H), 3.82–3.75 (m, 2H), 3.58 (s, 3H), 3.55–3.51 (m, 2H), 3.45–3.14 (m, 9H), 2.92–2.75 (m, 2H), 2.37–2.29 (m, 3H), 2.16–2.01 (m, 2H), 1.85–1.44 (m, 11H); ^{13}C NMR (151 MHz, $CDCl_3$) δ 174.12, 168.84, 151.32, 129.08, 119.61, 116.02, 62.75, 62.11, 56.75, 56.45, 53.51, 51.48, 48.96, 44.56, 39.87, 34.95, 33.88, 32.61, 29.70, 29.22, 28.29, 27.22, 25.55, 21.98, 21.09, 14.12. IR (KBr) ν: 3415, 2956, 2854, 1723, 1657, 1456, 1384, 1261, 1020, 748, 681; HR-MS (ESI) m/z: Calculated for $C_{28}H_{43}N_4O_3$ $[M + H]^+$ ms: 483.3330 found: 483.3329.

M2: yellow powder; yield: 63%; m.p.: 192–194 °C; ^{1}H NMR (600 MHz, DMSO-d6) δ: 10.07 (d, J = 4.8 Hz, 2H), 7.37 (t, J = 8.4 Hz, 2H), 7.02 (d, J = 8.4 Hz, 2H), 6.87 (t, J = 8.4 Hz, 1H), 4.82–4.79 (m, 1H), 4.40 (d, J = 15.6 Hz, 1H), 4.20–4.15 (m, 1H), 3.82–3.75 (m, 2H), 3.58–3.52 (m, 4H), 3.45 (d, J = 7.2 Hz, 1H), 4.04 (q, J = 7.2 Hz, 2H), 3.39–3.11 (m, 7H), 2.93–2.77 (m, 2 H), 2.38–2.24 (m, 3H), 2.16–2.01 (m, 2H), 1.91–1.80 (m, 1H), 1.76–1.60 (m, 7H), 1.56–1.42 (m, 3H), 1.17 (t, J = 7.2 Hz, 3H). ^{13}C NMR (151 MHz, $CDCl_3$) δ 173.71, 168.96, 151.28, 129.08, 119.65, 116.04, 62.94, 61.97, 60.22, 56.61, 56.36, 53.84, 53.47, 48.94, 44.79, 39.73, 35.05, 34.12, 32.39, 31.91, 30.31, 29.69, 28.95, 28.01, 21.96, 20.86, 14.26. IR (KBr) ν: 3412, 2955, 2860, 1722, 1662, 1472, 1274, 1042, 740, 688; HR-MS (ESI) m/z: Calculated for $C_{29}H_{45}N_4O_3$ $[M + H]^+$ ms: 497.3486 found: 497.3492.

M3: yellow powder; yield: 68%; m.p.: 187–189 °C; ^{1}H NMR (600 MHz, D_2O) δ: 7.00 (t, J = 7.8 Hz, 1H), 6.95 (d, J = 7.8 Hz, 1H), 6.88 (d, J = 8.4 Hz, 1H), 6.86 (t, J = 8.4 Hz, 1H), 4.32–4.30 (m, 1H), 4.16–4.13 (m, 1H), 4.03–3.99 (m, 1H), 3.76–3.01 (m, 16H), 2.80–2.67 (m, 2H), 2.35 (s, 1H), 2.27–2.16 (m, 2H), 2.00–1.94 (m, 1H), 1.76–1.32 (m, 12H), ^{13}C NMR (151 MHz, $CDCl_3$) δ 174.18, 169.04, 152.28, 141.41, 122.83, 120.96, 118.19, 111.21, 62.77, 62.13, 56.77, 56.47, 55.37, 53.78, 51.47, 50.47, 44.55, 39.96, 35.02, 33.91, 32.60, 29.70, 29.21, 28.28, 27.22, 22.69, 21.99, 21.13, 14.12. IR (KBr) ν: 3424, 2936, 2858, 1729, 1647, 1470, 1378, 1258, 1024, 837; HR-MS (ESI) *m/z*: Calculated for $C_{29}H_{45}N_4O_4$ $[M + H]+$ ms: 513.3435 found: 513.3438.

M4: yellow powder; yield: 62%; m.p.: 193–195 °C; ^{1}H NMR (600 MHz, D_2O) δ: 7.07 (t, J = 7.8 Hz, 1H), 7.02 (d, J = 7.8 Hz, 1H), 6.92 (d, J = 8.4 Hz, 1H), 6.86 (t, J = 7.8 Hz, 1H), 4.33–4.30 (m, 1H), 4.36–4.33 (m, 1H), 4.17–4.14 (m, 1H), 4.02–3.98 (m, 1H), 3.93 (q, J = 7.2 Hz, 2H), 3.69 (s, 3H), 3.57–3.26 (m, 11H), 3.13–3.02 (m, 3H), 2.80–2.69 (m, 2H), 2.34 (s, 1H), 2.25–2.16 (m, 2H), 2.00–1.92 (m, 1H), 1.73–1.32 (m, 12H), 1.02 (t, J = 7.2 Hz, 1H); ^{13}C NMR (151 MHz, $CDCl_3$) δ 173.75, 169.05, 152.28, 141.39, 122.84, 120.96, 118.19, 111.20, 62.78, 62.10, 60.19, 56.77, 56.46, 55.36, 53.77, 50.46, 44.60, 39.87, 34.97, 34.18, 32.58, 31.93, 29.70, 29.18, 28.29, 27.21, 22.69, 22.02, 21.10, 14.26. IR (KBr) ν: 3437, 2926, 2846, 1733, 1631, 1463 1278, 1233, 1028, 831; HR-MS (ESI) *m/z*: Calculated for $C_{30}H_{47}N_4O_4$ $[M + H]^+$ ms: 527.3592 found: 527.3598.

M5: yellow powder; yield: 64%; m.p.: 193–196 °C; ^{1}H NMR (600 MHz, D_2O) δ: 7.14 (t, J = 7.8 Hz, 1H), 6.55 (d, J = 7.8 Hz, 1H), 6.49 (d, J = 7.8 Hz, 1H), 6.48 (s, 1H), 4.10–3.97 (m, 2H), 3.90–3.79 (m, 1H), 3.67 (s, 3H), 3.51–3.49 (m, 1H), 3.47 (s, 3H), 3.37–2.85 (m, 12H), 2.80–2.69 (m, 2H), 2.33 (s, 1H), 2.25–2.18 (m, 2H), 2.02–1.92 (m, 1H), 1.84–1.32 (m, 12H); IR (KBr) ν: 3419, 2940, 2843, 2730, 1729, 1656, 1464, 1389, 1253, 1028, 826; ESI-MS, *m/z*: 513 {(M + 1)}.

M6: yellow powder; yield: 61%; m.p.: 188–191 °C; ^{1}H NMR (600 MHz, D_2O) δ: 6.95 (d, J = 9.0 Hz, 2H), 6.93 (d, J = 9.0 Hz, 2H), 4.33–4.31 (m, 1H), 4.15–4.12 (m, 1H), 4.02–3.98 (m, 1H), 3.69 (s, 3H), 3.51–3.02 (m, 16H), 2.80–2.69 (m, 2H), 2.35 (s, 1H), 2.27–2.16 (m, 2H), 2.01–1.92 (m, 1H), 1.77–1.31 (m, 12H); IR (KBr) ν: 3427, 2912, 2836, 1723, 1629, 1465, 1282, 1233, 1025, 851; ESI-MS, *m/z*: 513 {(M + 1)}.

M7: yellow powder; yield: 63%; m.p.: 189–191 °C; ^{1}H NMR (600 MHz, D_2O) δ: 7.13 (t, J = 8.4 Hz, 1H), 6.95 (s, 1H), 6.85 (d, J = 8.4.0 Hz), 6.82 (d, J = 8.4 Hz,), 4.32–4.29 (m, 1H), 4.15–4.10 (m, 1H), 4.03–3.99 (m, 1H), 3.82–3.00 (m, 16H), 2.80–2.70 (m, 2H), 2.34 (s, 1H), 2.34–2.24 (m, 2H), 2.00 –1.97 (m, 1H), 1.76–1.30 (m, 12H); IR (KBr) ν: 3424, 2939, 2858, 1719, 1657, 1461, 1387, 1269, 1021, 757, 691; ESI-MS, *m/z*: 517 {(M + 1)}.

M8: yellow powder; yield: 65%; m.p.: 189–192 °C; ^{1}H NMR (600 MHz, D_2O) δ: 7.13 (t, J = 8.4 Hz, 1H), 6.95 (s, 1H), 6.85 (d, J = 8.4 Hz), 6.82 (d, J = 8.4.0 Hz), 4.20–4.17 (m, 1H), 4.06–3.91 (m, 1H), 3.92 (q, J = 7.2 Hz, 2H), 3.67 (s, 3H), 3.62–3.15 (m, 11H), 3.12–3.01 (m, 3H), 2.78–2.65 (m, 2H), 2.34 (s, 1H), 2.25–2.15 (m, 2H), 2.01–1.94 (m, 1H), 1.75–1.34 (m, 12H), 1.02 (t, J = 8.4 Hz, 3H); IR (KBr) ν: 3423, 2936, 2857, 1731, 1654, 1489, 1456, 1399, 1261, 1026, 744, 686; ESI-MS, *m/z*: 542.45 {$(M + Na^+)$}.

M9: yellow powder; yield: 64%; m.p.: 188–192 °C; ^{1}H NMR (600 MHz, D_2O) δ: 6.94 (d, J = 7.2 Hz, 2H), (d, J = 7.2 Hz, 2H) 4.23–4.20 (m, 1H), 4.11–3.93 (m, 2H), 3.63–3.49 (m, 1H), 3.69 (s, 3H), 3.51–3.02 (m, 12H), 2.80–2.70 (m, 2H), 2.34 (s, 1H), 2.26–2.17 (m, 2H), 2.01–1.92 (m, 1H), 1.69–1.33 (m, 12H); IR (KBr) ν: 3424, 2922, 2841, 1738, 1663, 1460, 1264, 1023, 741; ESI-MS, *m/z*: 501 {(M + 1)}.

M10: yellow powder; yield: 65%; m.p.: 184–186 °C; ^{1}H NMR (600 MHz, D_2O) δ: 7.04–6.95 (m, 4H), 4.34–4.31 (m, 1H), 4.16–4.12 (m, 1H), 4.03–3.99 (m, 1H), 3.93 (q, J = 7.2 Hz, 2H), 3.66–3.03 (m, 13H), 2.81–2.70 (m,2H), 2.35 (s, 1H), 2.24–2.18 (m, 2H), 2.02–1.92 (m, 1H), 1.77–1.32 (m, 12H), 1.03 (q, J = 7.2 Hz, 3H); IR (KBr) ν: 3427, 2959 2857, 2748, 1729, 1658, 1495, 1466, 1390, 1257, 1027,740; ESI-MS, *m/z*: 515 {(M + 1)}.

M11: yellow powder; yield: 62%; m.p.: 189–193 °C; ^{1}H NMR (600 MHz, D_2O) δ: 7.14 (t, J = 7.8 Hz, 1H), 6.54 (d, J = 7.8 Hz, 1H), 6.47 (d, J = 7.8 Hz, 1H), 6.48 (s, 1H), 4.33–4.35 (m, 1H), 4.15–4.12 (m, 1H), 4.06–3.98 (m, 1H), 3.92 (q, J = 7.2 Hz, 2H), 3.67 (s, 3H), 3.62–3.15 (m, 11H), 3.12–3.01 (m, 3H), 2.78–2.65 (m, 2H), 2.35 (s, 1H), 2.25–2.16 (m, 2H), 2.01–1.93 (m, 1H), 1.76–1.34 (m, 12H), 1.04 (t, J = 8.4 Hz, 1H); IR (KBr) ν: 3431, 2925, 2836, 1723, 1629, 1465, 1278, 1233, 1026, 843; ESI-MS, *m/z*: 515 {(M + 1)}.

M12: yellow powder; yield: 66%; m.p.: 189–192 °C; ^{1}H NMR (600 MHz, D_2O) δ: 7.05 (t, J = 7.8 Hz, 1H), 7.03 (d, J = 7.8 Hz, 1H), 6.99 (d, J = 8.4 Hz, 1H), 6.62 (t, J = 7.8 Hz, 1H), 4.34–4.31 (m, 1H), 4.15–4.11 (m, 1H), 4.02–3.98 (m, 1H), 3.93 (q, J = 7.2 Hz, 2H), 3.69 (s, 3H), 3.62–3.15 (m, 11H), 3.13–3.02 (m, 3H), 2.80–2.69 (m, 2H), 2.34 (s, 1H), 2.25–2.16 (m, 2H), 2.00–1.92 (m, 1H), 1.75–1.33 (m, 12H), 1.03 (t, J = 8.4 Hz, 1H); IR (KBr) ν: 3441, 2931, 2841, 1729, 1643, 1462, 1269, 1237, 1026, 743; ESI-MS, *m/z*: 515 {(M + 1)}.

M13: yellow powder; yield: 61%; m.p.: 190–192 °C; ^{1}H NMR (600 Hz, DMSO-d6) δ: 10.06–9.88 (m, 1H), 7.91 (d, J = 8.4 Hz, 1H), 7.69 (m, 1H), 7.42 (d, J = 8.4 Hz, 1H), 7.26 (m, 1H), 4.82–4.80 (m, 1H), 4.34 (d, J = 15.6 Hz, 1H), 4.21–4.12 (m, 2H), 3.58 (s, 3H), 3.56–3.52 (m, 2H), 3.51–3.47 (m, 1H), 3.45–3.41 (m, 2H), 3.38–3.24 (m, 6H), 2.91–2.77 (m, 2H), 2.39–2.28 (m, 3H), 2.15–2.03 (m, 2H), 1.88–1.81 (m, 1H), 1.76–1.46 (m, 10H); IR (KBr) ν: 3422, 2958, 2860, 1722, 1682, 1461, 1269, 1032, 746; ESI-MS, *m/z*: 527.77 {(M + 1)}.

M14: yellow powder; yield: 67%; m.p.: 182–185 °C; ^{1}H NMR (600 MHz, D_2O) δ: 7.79 (d, J = 8.4 Hz, 1H), 7.50 (t, J = 8.4 Hz, 1H), 7.22 (d, J = 8.4 Hz, 1H), 7.11 (t, J = 8.4 Hz, 1H), 4.32–4.29 (m, 1H), 4.13–4.09 (m, 1H), 4.02–3.98 (m, 1H), 3.79–3.50 (m, 3H), 3.48 (s, 3H), 3.44–2.99 (m, 10H), 2.80–2.69 (m, 2H), 2.33 (s, 1H), 2.25–2.18 (m, 2H), 2.02–1.92 (m, 1H), 1.81–1.29 (m, 12H), 1.03 (t, J = 8.4 Hz, 3H); IR (KBr) ν: 3423, 2936, 2857, 1731, 1654, 1489, 1456, 1399, 1261, 1026, 744, 686; ESI-MS, *m/z*: 542 {(M + 1)}.

M15: yellow powder; yield: 68%; m.p.: 188–192 °C; ^{1}H NMR (600 MHz, DMSO-d6) δ: 10.02–9.97 (s, 2H), 7.12 (d, J = 9.6 Hz, 2H), 6.87 (d, J = 9.6 Hz, 1H), 4.81–4.80 (m, 1H), 4.32 (m, 1H), 4.21–4.16 (m, 2H), 4.10 (m, 1H), 3.58 (s, 3H), 3.57–3.39 (m, 7H), 3.36–3.25 (m, 2H), 3.21–3.13 (m, 2H), 2.92–2.78 (m, 2H), 2.40–2.25 (m, 3H), 2.15–2.05 (m, 2H), 1.84–1.24 (m, 11H); IR (KBr) ν: 3431, 2971, 2859, 1734, 1678, 1459, 1275, 1044, 821; ESI-MS, *m/z*: 528.40 {(M + 1)}.

M16: yellow powder; yield: 61%; m.p. 186–188 °C; ^{1}H NMR (600 Hz, D_2O) δ: 7.33 (t, *J* = 7.8 Hz, 1H), 7.19 (s, 1H), 7.14 (d, *J* = 7.8 Hz, 1H), 7.12 (d, *J* = 7.8 Hz, 1H), 4.33–4.29 (m, 1H), 4.15– 4.10 (m, 1H), 4.03–3.99 (m, 1H), 3.82–3.00 (m, 16H), 2.80–2.70 (m, 2H), 2.35 (s, 1H), 2.34–2.24 (m, 2H), 2.00–1.97 (m, 1H), 1.75–1.32 (m, 12H); IR (KBr) ν: 3417, 2947, 2863, 2738, 1719, 1656, 1494, 1460, 1389, 1247, 1025, 748, 692; ESI-MS, *m/z*: 551 {(M + 1) };

M17: yellow powder; yield: 58%; m.p.: 184–187 °C; ^{1}H NMR (600 MHz, D_2O) δ: 7.38 (t, J = 7.2 Hz, 1H), 7.32 (t, J = 7.2 Hz, 2H), 7.28 (d, J = 7.2 Hz, 2H), 4.32–4.29 (m, 1H), 4.13–4.09 (m, 1H), 4.01–3.97 (m, 1H), 3.86–3.00 (m, 16H), 2.79–2.69 (m, 2H), 2.34 (s, 1H), 2.27–2.15 (m, 2H), 2.00–1.91 (m, 1H), 1.68–1.36 (m, 12H); IR (KBr) ν: 3451, 2948, 2834, 1731, 1640, 1481, 1379, 1242, 1037, 754, 700; ESI-MS, *m/z*: 511 {(M + 1)}.

M18: yellow powder; yield: 56%; m.p.: 185–187 °C; ^{1}H NMR (600 MHz, D_2O) δ: 7.38 (t, J = 7.2 Hz, 1H), 7.33 (t, J = 7.2 Hz, 2H), 7.28 (d, J = 7.2 Hz, 2H), 4.32–4.29 (m, 1H), 4.13–4.09 (m, 1H), 4.01–3.97 (m, 1H), 3.92 (q, J = 7.2 Hz, 2H), 3.82–2.99 (m, 14H), 2.79–2.69 (m, 2H), 2.34 (s, 1H), 2.27–2.15 (m, 2H), 2.00–1.91 (m, 1H), 1.68–1.36 (m, 12H), 1.02 (t, J = 7.2 Hz, 3H); IR (KBr) ν: 3443, 2936, 2837, 1742, 1659, 1486, 1462, 1367, 1239, 1031, 750, 703; ESI-MS, *m/z*: 525 {(M + 1)}.

M19: yellow powder; yield: 53%; m.p.: 185–188 °C; ^{1}H NMR (600 MHz, D_2O) δ: 7.28 (d, J = 8.4 Hz, 2H), 6.88 (d, J = 8.4 Hz, 2H), 4.32–4.29 (m, 1H), 4.25–4.22 (m, 1H), 4.13–4.08 (m, 1H), 4.01–3.97 (m, 1H), 3.67 (s, 3H), 3.6–3.53 (m, 1H), 3.46 (s, 3H), 3.39–2.97 (m, 10H), 2.88–2.82 (m, 1H), 2.79–2.63 (m, 2H), 2.34 (s, 1H), 2.23–2.16 (m, 2H), 1.98–1.91 (m, 1H), 1.68–1.32 (m, 12H); IR (KBr) ν: 3423, 2937, 2861, 1721, 1655, 1479, 1450, 1391, 1261, 1027, 744; ESI-MS, *m/z*: 541 {(M + 1)}.

M20: yellow powder; yield: 55%; m.p.: 184–186 °C; ^{1}H NMR (600 MHz, DMSO-d6) δ: 10.02–9.97 (m, 2H), 7.07 (t, J = 7.8 Hz, 1H), 7.02 (d, J = 7.8 Hz, 1H), 6.92 (d, J = 8.4 Hz, 1H), 6.86 (t, J = 7.8 Hz, 1H), 4.81 (m, 1H), 4.32 (m, 1H), 4.22–4.15 (m, 2H), 4.10 (m, 1H), 3.58 (s, 3H), 3.57–3.39 (m, 7H), 3.36–3.25 (m, 2H), 3.21–3.13 (m, 2H), 2.92–2.78 (m, 2H), 2.44–2.27 (m, 3H), 2.14–2.05 (m, 2H), 1.91–1.24 (m, 11H); IR (KBr) ν: 3453, 2952, 2834, 1741, 1644, 1485, 1379, 1245, 1073, 755; ESI-MS, *m/z*: 529 {(M + 1)}.

M21: yellow powder; yield: 59%; m.p. 181–183 °C; ^{1}H NMR (600 MHz, D_2O) δ: 8.20 (d, J = 8.4 Hz, 1H), 8.17 (s, 1H), 7.69 (d, J = 8.4 Hz, 1H), 7.56 (t, J = 8.4 Hz, 1H), 4.25–4.22 (m, 1H), 4.12–4.08 (m, 1H), 4.00–3.97 (m, 1H),

3.6–3.53 (m, 1H), 3.46 (s, 3H), 3.39–2.97 (m, 10H), 2.88–2.82 (m, 1H), 2.79–2.63 (m, 2H), 2.34 (s, 1H), 2.26–2.16 (m, 2H), 1.98–1.93 (m, 1H), 1.64–1.32 (m, 12H); IR (KBr) ν: 3452, 2943, 2837, 1732, 1649, 1481, 1399, 1261, 1027,756; ESI-MS, *m/z*: 556 {(M + 1)}.

M22: white powder; yield: 54%; m.p.: 175–177 °C; ^{1}H NMR (600 MHz, D_2O) δ: 8.94 (s, 1H), 8.79 (s, 1H), 8.70 (d, J = 5.4 Hz, 1H), 8.39 (d, J = 8.4 Hz, 1H), 7.88 (t, J = 7.8 Hz, 1H), 4.48–4.44 (m, 1H), 4.27–4.22 (m, 1H), 4.10–4.04 (m, 1H), 4.03–3.07 (m, 16H), 2.88–2.77 (m, 2H), 2.44 (s, 1H), 2.34–2.24 (m, 2H), 3.09–3.03 (m, 1H), 2.3–2.15 (m, 2H), 1.83–1.40 (m, 12H); IR (KBr) ν: 3436, 2943, 2846, 1731, 1654, 1474, 1379, 1247, 1038, 743, 709; ESI-MS, *m/z*: 512 {(M + 1)}.

M23: white powder; yield: 52%; m.p.: 183–186 °C; ^{1}H NMR (600 MHz, D_2O) δ: 8.83 (s, 1H), 8.73 (d, J = 5.4 Hz, 1H), 8.49 (d, J = 8.4 Hz, 1H), 7.96 (t, J = 7.8 Hz, 1H), 4.37–4.38 (m, 1H), 4.18–4.12 (m, 2H), 4.01–2.96 (m, 13H), 2.79–2.69 (m, 2H), 2.34 (s, 1H), 2.23–2.15 (m, 2H), 2.97 (s, 1H), 2.23–2.15 (m, 2H), 1.75–1.31 (m, 12H), 1.02 (t, J = 7.2 Hz, 3H); IR (KBr) ν: 3433, 2946, 2847, 1737, 1644, 1484, 1459, 1389, 1257, 1025, 744; ESI-MS, *m/z*: 526 {(M + 1) }.

M24: white powder; yield: 51%; m.p. 172–175 °C; ^{1}H NMR (600 MHz, D_2O) δ: 7.52 (d, J = 4.8 Hz, 1H), 7.29 (d, J = 3.6 Hz, 1H), 6.98 (t, J = 4.2 Hz, 1H), 4.33–4.30 (m, 1H), 4.26–4.23 (m, 1H), 4.14–4.11 (m, 1H), 4.02–3.98 (m, 1H), 3.74–3.00 (m, 15H), 2.80–2.69 (m, 2H), 2.34 (s, 1H), 2.24–2.17 (m, 2H), 2.00–1.92 (m, 1H), 1.68–1.32 (m, 12H); IR (KBr) ν: 3443, 2936, 2852, 1726, 1647, 1485, 1455, 1376, 1252, 1029, 750, 689; ESI-MS, *m/z*: 517 {(M + 1)}.

M25: white powder; yield: 48%; m.p.: 175–179 °C; ^{1}H NMR (600 MHz, D_2O) δ: 7.52 (d, J = 4.8 Hz, 1H), 7.29 (d, J = 3.6 Hz, 1H), 6.98 (t, J = 4.2 Hz, 1H), 4.33–4.30 (m, 1H), 4.14–4.12 (m, 1H), 4.02–3.98 (m, 1H), 3.93 (q, J = 7.2 Hz, 2H), 3.79–2.98 (m, 11H), 2.80–2.68 (m, 2H), 2.34 (s, 1H), 2.22–2.18 (m, 2H), 2.00–1.93 (m, 1H), 1.68–1.32 (m, 12H), 1.02 (t, J = 7.2 Hz, 3H); IR (KBr) ν: 3443, 2941, 2849, 1727, 1645, 1474, 1381, 1257, 1029, 746, 706; ESI-MS, *m/z*: 531 {(M + 1)}.

Synthesis of compounds M26, M27

Compound **M13/M16** was dissolved in a mixture aqueous of NaOH aqueous (1 M) and 1, 4-dioxane.The reaction mixture was then stirred at room temperature for 1 h. Diluted hydrochloric acid was added to neutralize the above solution to pH 6~7, followed by its extraction with diethyl ether (3 × 20 mL). The organic layer was collected, dried with sodium sulfate, filtered and evaporated under vacuum to obtain crude products. The products were further purified by column chromatography on silica gel eluting with dichloromethane: methanol (10:1~5:1) to afford oil products. Then saturated solution of hydrochloric acid in ethanol was added to the products and mixture was concentrated to get final target compounds **M26**, **M27**.

M26: yellow powder; yield: 47%; m.p.: 191–193 °C; ^{1}H NMR (600 MHz, D_2O) δ: 7.57 (d, J = 8.5 Hz, 2H), 7.14 (d, J = 9.7 Hz, 2H), 4.34–4.31 (m, 1H), 4.14–4.10 (m, 1H), 4.03–3.98 (m, 1H), 3.67–2.02 (m, 13 H), 2.88–2.82 (m, 1H), 2.80–2.69 (m, 2H), 2.34 (s, 1H), 2.24–2.15 (m, 2H), 2.01–1.96 (m, 1H), 1.68–1.32 (m, 12H); IR (KBr) ν: 3425, 2939, 2861, 1737, 1658, 1495, 1466, 1387, 1252, 1024, 745, 687; ESI-MS, *m/z*: 537.44 {(M + 1)}.

M27: yellow powder; yield: 45%; m.p.: 187–189 °C; ^{1}H NMR (600 MHz, D_2O) δ: 7.80 (d, J = 8.4 Hz, 1H), 7.49 (t, J = 8.4 Hz, 1H), 7.22 (d, J = 8.4 Hz, 1H), 7.11 (t, J = 8.4 Hz, 1H), 4.35–4.27 (m, 1H), 4.13–4.11 (m, 1H), 4.08–3.05 (m, 1H), 3.81–3.51 (m, 3H), 3.48 (s, 3H), 3.44–2.99 (m, 10H), 2.82–2.69 (m, 2H), 2.34 (s, 1H), 2.26–2.19 (m, 2H), 2.03–1.93 (m, 1H), 1.83–1.31 (m, 12H); IR (KBr) ν: 3432, 2855, 1725, 1692, 1465, 1251, 1028, 741; ESI-MS, *m/z*: 514.35 {(M + 1)}.

Cell viability assay

The cell viability of the prepared compounds against Bel-7402 and RKO cell lines was evaluated. The suspension (100 µL/well) with evaluated cells (3~4 × 10^4 cell/mL) and DMEM culture medium of 10% fetal bovine serum (FBS) were seeded into 96-well plates. The subsequent incubation was performed for 24 h at 37 °C under a 5% CO_2 atmosphere prior to the cytotoxicity assessments. Target compounds with concentration of 50 µM, made by dilution in culture medium (DMEM of 10% fetal bovine serum) of stock solutions of test compounds prepared in DMSO, were added and incubated for 48 h. Supernatant from each well was carefully removed and 30 µL PBS containing 2.5 mg·mL^{-1} MTT was added to each well. After 4 h, 100 µL DMSO was added to each well for the colorimetric reaction. Finally, the optical density was measured at 570 nm wavelength on an enzyme-linked immunosorbent assay microplate reader. Three replicate wells were used for each drug concentration in all experiments. Each assay was performed at least three times. The cell viability of test substances was calculated using the below equation:

$$\text{Cell viability}(\%) = \text{OD value of given drug group} / \text{OD value of control group} \times 100\%$$

Antitumor activity in vivo

Tumor-bearing mice were prepared by inoculating a suspension of H22 cells (5 × 10^6 cells per mouse) subcutaneously into the right armpit of each mouse, nine days

inoculation, according to body weight, mice were assigned to equal groups: i.e., Cyclophosphamide group (positive control, 30 mg/kg), vehicle group (60 mg/kg), 27 given drug groups (60 mg/kg) and matrine group (negative control, 60 mg/kg). All treatments were administered for 10 days. One day after, mice were sacrificed, the body, thymus, spleen and tumor weight (g) were measured. The toxicity of drugs was demonstrated by their thymus index and spleen index by comparing with that of vehicle group. The discrepancy of tumor weight between drugs group and vehicle group indicated the antitumor efficiency in vivo. The inhibition was calculated as follows: inhibition (%) = [1 − (mean tumor weight of tested mice)/(mean tumor weight of control mice] × 100.

Data accessibility

The datasets supporting this article have been uploaded as part of the electronic supplementary material.

Acknowledgements We are grateful to Prof. Chen Rui, Faculty of Chinese Medicine Science, Guangxi University of Chinese Medicine for proofreading of the manuscript.

Author contributions Y.X. and P.L. performed research and drafted the initial manuscript. H.R. revised and approved the manuscript. L.W. helped in biological activity. P.X modified the language. H.W. and S. Z. contributed the compounds synthesis. L.W. and J.J. designed the research.

Funding This work was supported by the National Natural Science Foundation of China (21403225), the Innovation Project of Guangxi Graduate Education (YCBZ2019026), the high-level innovation team and outstanding scholar project of Guangxi institutions of higher education (guijiaoren (2014) 49 hao), Guangxi Natural Science Foundation (2017GXNSFBA198240) and the State Key Laboratory for Chemistry and Molecular Engineering of Medicinal Resources, Guangxi Normal University (CMEMR2017-B14).

Compliance with ethical standards

Conflict of interest The authors declare that they have no conflict of interest.

Ethics approval Mice were purchased from Beijing Vital River Laboratory Animal Technology Co., Ltd. (Beijing, China). All protocols and care of the mice were performed in strict compliance with Guidelines for the Use of Laboratory Animals (National Research Council) and approved by the SPF Animal Laboratory of Guangxi University.

Publisher's note: Springer Nature remains neutral with regard to jurisdictional claims in published maps and institutional affiliations.

References

Aghvami M, Ebrahimi F, Zarei MH et al. (2018) Matrine induction of ROS mediated apoptosis in human ALL B-lymphocytes Via mitochondrial targeting. Asian Pac J Cancer Prev 19:555–560

Dai Z-J, Gao J, Ji Z-Z, Wang X-J, Ren H-T, Liu X-X, Wu W-Y, Kang H-F, Guan H-T (2009) Matrine induces apoptosis in gastric carcinoma cells via alteration of Fas/FasL and activation of caspase-3 J Ethnopharmacol 123:91–96

Fajas L, Benfodda Z, Fritz V (2011) Preparation of piperazine derivatives as inhibitors of stearoyl-CoA-desaturase-1enzyme. WO 2011/030312 A1. 2011.

Hamdy AA (2012) Cancer therapy and vaccination. J Immunol Methods 382:1–23

Jones P, Maria Ontoria OJ (2011) Preparation of piperidine and piperazine derivatives as SMO antagonist. WO 2011/036478 A1. 2011.

Kimura M, Masuda T, Yamada K, Kawakatsu N, Kubota N, Mitani M, Kishii K, Inazu M, Kiuchi Y, Oguchi K, Namiki T (2004) Antioxidative activities of novel diphenylalkyl piperazine derivatives with high affinities for the dopamine transporter. Bioorg Med Chem Lett 14:4287–4290

Lacivita E, Leopoldo M, De Giorgio P, Berardi F, Perrone R (2009) Determination of 1-aryl-4-propylpiperazine pKa values: the substituent on aryl modulates basicity. Bioorg Med Chem 17:1339–1344

Lin Y, Lin L, Jin Y, Wang D, Tan Y, Zheng C (2014) Combination of matrine and sorafenib decreases the aggressive phenotypes of hepatocellular carcinoma cells. Chemotherapy 60:112–118

Rathi AK, Syed R, Shin H-S, Patel RV (2016) Piperazine derivatives for therapeutic use: a patent review (2010-present). Expert Opin Ther Pat 26:777–797

Schiemann K, Schultz M, Staehle W (2010) Piperidine and piperazine derivatives as autotaxin inhibitors and their preparation and use for the treatment and prophylaxis of cancers and other autotaxin-mediated diseases. WO 2010115491 A2. 2010.

Shapiro LA, Offord SJ, Ordway GA (1995) The effect of chronic treatment with a novel aryl-piperazine antipsychotic on monoamine receptors in rat brain. Brain Res 677:250–260

Solomon VR, Hu C, Lee H (2010) Design and synthesis of anti-breast cancer agents from 4-piperazinylquinoline: a hybrid pharmacophore approach. Bioorg Med Chem 18:1563–1572

Yang C, Xu G, Li J, Wu X, Liu B, Yan X, Wang M, Xie Y (2005) Benzothiophenes containing a piperazine side chain as selective ligands for the estrogen receptor α and their bioactivities in vivo. Bioorg Med Chem Lett 15:1505–1507

Zhang GL, Jiang L, Yan Q, Liu RH, Zhang L (2015) Anti-tumor effect of matrine combined with cisplatin on rat models of cervical cancer. Asian Pac J Trop Med 8:1055–1059

Zhang JQ, Li YM, Liu T et al. (2010) Antitumor effect of matrine in human hepatoma G2 cells by inducing apoptosis and autophagy. World J Gastroenterol 16:4281–4290